Submitted to Review on Advanced Materials Science (February 2017)

Evolution of homogeneity in oxygen-free copper processed by either ECAP or HPT

Meshal Alawadhi[a], Yi Huang[a,*] and Terence. G. Langdon[a]

[a]Materials Research Group, Faculty of Engineering and the Environment, University of Southampton, Southampton SO17 1BJ, UK

*Corresponding author: y.huang@soton.ac.uk (Yi Huang)

Abstract

Oxygen-free copper having a commercial purity of 99.95 wt.% was processed at room temperature by severe plastic deformation (SPD) using either equal-channel angular pressing (ECAP) or high-pressure torsion (HPT). The ECAP billets were processed through a die having an internal angle of 110° for up to 8 passes and the HPT discs were processed under an applied pressure of 6.0 GPa for up to 10 turns. The evolution of microstructural homogeneity was investigated for each process by measuring the grain sizes and recording the distributions of the microhardness values on the cross-sectional planes of the ECAP billets and on the disc surface planes of the HPT samples. For both sets of measurements, the hardness values were recorded following a rectilinear grid pattern in order to generate colour-coded maps of the hardness distributions.

Keywords: Copper; Equal-channel angular pressing; High-pressure torsion; Microhardness; Severe plastic deformation.

1. Introduction

Over the last two decades, severe plastic deformation (SPD) has been used successfully for the production of ultrafine-grained (UFG) materials having grains in the range of submicrometer or nanometer sizes [1-4]. It is now well established that materials with very small grain sizes exhibit high strength at low temperatures as expressed by the Hall-Petch relationship [5,6]. Although several different SPD processing techniques are now available, most attention to date has focused on the procedures of equal-channel anglular pressing (ECAP) or high-pressure torsion (HPT) [7]. In ECAP a rod or bar is pressed through a die constrained within a channel that is bent through a sharp angle within the die [8]. In HPT the sample, generally in the form of a thin disc, is subjected to a high applied pressure and concurrent torsional straining [9]. Both of these methods are effective in producing exceptional grain refinement but HPT has the advantage that, by comparison with ECAP, it produces a smaller grain size [10,11] and a higher fraction of grain boundaries having high angles of misorientation [12].

The extent of the strengthening of metals by SPD is most effectively measured by recording the hardness values after processing. There are now many reports of hardness measurements after SPD with the values recorded on different sectional planes within the samples. In ECAP, the hardness values are generally measured on cross-sectional planes cut perpendicular to the pressing direction [13] but there are also reports of measurements on longitudinal planes along the lengths of the billets [14]. In HPT, hardness measurements are generally recorded on the upper surface after processing [15,16] but there are also reports of measurements on planes cut vertical to the disk upper surfaces [17] and on various planes cut parallel to the upper surface [18]. All of these results confirm that there is a reasonable level of hardness homogeneity in the billets processed by ECAP whereas in HPT the situation is more complex because the strain varies across the disc diameter and this leads initially to

inhomogeneities in both the hardness and the microstructure. By processing HPT disks through fractional numbers of turns such as 1/8 and 1/4 turn, it was established that the hardness gradually evolves with increasing strain to produce a reasonable level of homogeneity [19]. This evolution has been explained theoretically using strain gradient plasticity [20] and the development of a hardness evolution has been examined and summarized for a large number of metallic systems [21].

The present investigation was prompted by the recognition that most reports of hardness evolution in ECAP or HPT relate to the use of different materials, or possibly even to similar materials but obtained from different sources, in order to document the individual hardness values and the gradual evolution with straining. This use of different materials makes it difficult to obtain an accurate assessment of the true differences between the hardness evolution in ECAP and HPT. Accordingly, the present investigation was initiated specifically to make use of the same material, oxygen-free copper of commercial purity, for processing by either ECAP or HPT and by conducting all processing at room temperature to avoid any thermal effects. Oxygen-free copper was selected as the test material both because of the interests in using this material in industrial applications and because of very recent reports demonstrating the development of unusual effects in the hardness evolution in this material in the earliest stages of HPT processing [22-24].

2. Experimental material and procedures

The experiments were conducted using a commercial oxygen-free copper having a purity of 99.95%. Each ECAP billet was ~65 mm long with a diameter of 10 mm and each HPT disc had a diameter of 10 mm and a thickness of ~0.83 mm. Both the billets and the discs were initially annealed for one hour at a temperature of 600°C using a vacuum tube furnace. In

the annealed condition, the unprocessed material had a measured average Vickers microhardness of Hv ≈ 41 and an average grain size of ~24 μm.

For ECAP, the billets were pressed through a solid die within a channel bent through an internal angle of $\Phi = 110^{o}$ and with an outer arc of curvature at the intersection of the two parts of the channel of $\Psi = 20^{o}$. These angles impose a strain on the sample of ~0.8 on each pass through the die [25]. The billets were pressed at room temperature using a plunger made of H13 tool steel through totals of 1, 2, 4, 6 and 8 passes. All billets were processed using route B_C in which the sample is rotated by 90° in the same direction around the longitudinal axis between each separate pass [26]. After processing by ECAP to the required number of passes, each billet was sectioned perpendicular to the pressing direction to reveal a cross-sectional plane near the centre of the billet.

The HPT facility consisted of upper and lower anvils having central depressions in the shape of circles with diameters of 10 mm and depths of 0.25 mm. Each disc was placed separately in the depression on the lower anvil and this anvil was then raised upwards to meet the depression in the upper anvil. The disc was compressed by an applied pressure of 6.0 GPa and torsional straining was imposed by rotating the lower anvil at a speed of 1 rpm. The applied pressure was maintained constant throughout the straining. The HPT processing was conducted using quasi-constrained conditions where there is a small space between the anvils that allows a limited outflow of material around the edge of the disc during processing [27,28]. The HPT discs were processed through different numbers of turns represented by N = 1/4, 1/2, 1, 3, 5 and 10 turns.

The ECAP planes of sectioning and the HPT discs were polished for microstructural observations and then Vickers microhardness measurements were taken using a Future-Tech microhardness tester, FM-300, by applying an indentation load of 100 gf for a dwell time of 15 s. These microhardness measurements were recorded over the exposed cross-sectional planes

of the ECAP billets and over the total surfaces of the HPT discs using a rectilinear grid pattern with a spacing between each separate indentation of 0.5 mm. The measured datum points were then used to construct colour-coded contour maps that offer a direct and simple visual display of the distributions of microhardness over the full surface of each specimen. For each sample, the average grain size was determined by taking measurements on EBSD images.

3. Experimental results

Following HPT processing, the average hardness and the grain size results are displayed in Fig. 1(a) where it is apparent that the hardness value increases significantly in the first 1/2 turn and at the same time the grain size decreases to within the submicrometer range. Thereafter, at larger numbers of turns, there is little or no significant change in either the microhardness or the grain size and thus both the hardness and the grain size reach saturation values at essentially the strain associated with 1/2 turn. The measured saturation values in the range of 5 to 10 HPT turns were a grain size of ~510 nm with an average microhardness of Hv ≈ 130,

Similar sets of data are shown in Fig. 1(b) for samples processed by ECAP. These results are similar to those obtained in HPT with increases in the microhardness and a corresponding decreaese in grain size but, due to the much lower strains imposed in ECAP, neither the microhardness nor the grain size attain true saturation values. Thus, the evidence suggests the microhardnes is continuing to slowly increase and the grain size is continuing to decreaese even after 8 passes of ECAP. In these experiments, the recorded average microhardness value after 8 passes was Hv ≈ 115 and the average grain size in this condition was ~2.9 μm. Thus, the straining in ECAP was insufficient to achieve a submicrometer grain size.

The results of the microhardness mapping after both HPT and ECAP are presented in Figs 2 and 3, respectively. All measurements were taken using a rectilinear grid pattern and the *X* and *Y* axes marked around the edges of each plot represent two orthogonal axes that were superimposed onto the polished surfaces so that the central point of each disc lies at the coordinates given by *X*, *Y* = (0,0). In Fig. 2 the results after HPT are shown for 1/4, 1, 5 and 10 turns and in Fig. 3 the results after ECAP are shown for 1, 2, 4 and 8 passes. The different colours denote differences in hardness values within the range from Hv ≈ 40 to 160 as denoted by the colour keys given on the right of each display with each separate colour representing an incremental step of 20.

A detailed inspection of Fig. 2(a) for 1/4 turn shows that there is initially an inhomogeneous microhardness distribution with a relatively large area of lower hardness values in the central region of the disc covering a diameter of approximately 2 mm. This is a reasonable result in the early stages of processing by HPT because the equivalent von Mises strain imposed on the disk, ε_{eq}, is given by a relationship of the form [29-31]:

$$\varepsilon_{eq} = \frac{2\pi Nr}{h\sqrt{3}} \qquad (1)$$

where *r* and *h* are the radius and height (or thickness) of the discc, respectively and *N* is the number of turns. Inspection of eq. (1) shows that the imposed strain varies across the disc such that the maximum value occurs at the outer edge and there is a strain equal to zero where *r* = 0 at the centre of each disc. This region of lower hardness shrinks to about 1 mm in diameter when the strain is increased to 1 turn as shown in Fig. 2(b) and at even higher numbers of turns, as in Figs 2(c) and (d), the central region of lower hardness essentially disappears and the whole surface of the disc shows a relatively similar level of microhardness with values of Hv ≈ 130.

Processing by ECAP is different because the imposed strains are much lower and there are no variations in strain across the diameters of the billets. Thus, Fig. 3 displays the hardness

distributions over the whole surfaces of the cross-sectional planes of the ECAP billets and in these images there is no evidence for an area of lower hardness in the central region or at any other region of the cross-sectional plane. In Fig. 3(a) there is relative homogeneity in the hardness distribution even after one pass of ECAP with an average microhardness value of Hv ≈110. It is also readily apparent from Fig. 3(b)-(d) that the hardness values gradually increase over the surfaces of these cross-sectional planes with increasing numbers of passes and ultimately they reach a value of Hv ≈115 throughout the sectional area after a total of 8 passes.

4. Discussion

The grain size measurements shown in Fig. 1 confirm that, as anticipated from earlier studies [10,11], ECAP and HPT both produce significant grain refinement in the early stages of processing but HPT leads to greater grain refinement and smaller grains. Thus, it is reasonable to anticipate from the Hall-Petch relationship that processing by HPT leads to higher strength

It is readily apparent from Figs 2 and 3 that the HPT discs show different microhardness evolutions compared with the ECAP billets because there are clear variations in the microhardness values across the HPT discs and this variation depends upon the number of revolutions and therefore the strain imposed by HPT. Thus, the microhardness values are lower at the centres of the discs than at the outer regions in the very early stages of HPT processing. Nevertheless, the microhardness increases and there is a gradual evolution towards homogeneity with increasing numbers of revolutions and torsional straining. This evolution is consistent with theoretical expectations [20] and it also matches earlier reports for microhardness evolution during HPT in pure copper [32] and a Cu-Zr alloy [33].

It is well established that the variation of hardness across the HPT discs is also related directly to the stacking fault energy (SFE) of the material since the SFE is the primary factor

controlling the nature of the recovery. Thus, materials with low SFE, where the separations between the partial dislocations are relatively large, tend to have slower recovery rates than materials with high SFE where the recombination of the partial dislocations occurs more easily. The initial lower hardness values in the central region of the oxygen-free copper discs processed by HPT in Fig. 2(a) are fully consistent with other studies on materials having similar SFE [33,34]. These studies show a gradual evolution towards hardness homogeneity with increasing torsional strain in the absence of any of the significant recovery that is well documented in high SFE materials such as pure Al [15].

For ECAP, the Vickers microhardness measurements were taken on the cross-sectional planes of billets and they demonstrate a very substantial increase in the average hardness value even after only one pass. This result matches early results reported for the ECAP processing of a number of commercial Al alloys [34]. It is apparent from Fig. 3(a) that there are variations in the hardness values over the cross-sectional plane but, unlike HPT, these variations are relatively minor and they are randomly distributed. Furthermore, the microhardness values increase with increasing numbers of passes so that there is a gradual evolution towards a high degree of microhardness homogeneity. These results are consistent with earlier reports for pure aluminium [35], aluminium alloys [35,36] and a copper alloy [37] processed by ECAP. By contrast, an Al-7034 alloy was processed by ECAP at a high temperature of 473 K for up to 6 passes and revealed a decrease in hardness after a single pass [38] where this weakening was due to a transformation of the metastable phase at the higher processing temperature of 473 K [39].

Although there are significant differences in the hardness values recorded across HPT discs in the early stages of processing, it was demonstrated in a very early analysis that the experimental points may be brought together in HPT by plotting all of the hardness datum points on a single plot against the equivalent strain [40]. To check this approach, and to extend

it also to the samples processed by ECAP, Fig. 4 shows the relationships between the measured microhardness values and the calculated equivalent strains for the samples processed by (a) HPT and (b) ECAP. The results for HPT in Fig. 4(a) are typical of a large number of alloys including samples where the HPT was conducted after processing by ECAP [41,42]. Thus, there is an initial increase in hardness but a saturation hardness of Hv ≈ 130 that is achieved at equivalent strains above ~35. The results for ECAP in Fig. 4(b) are similar but the saturation value is probably not fully achieved and the final maximum hardness is Hv ≈ 115. This behaviour is generally similar to the hardness model describing hardening without recovery after HPT processing [21]. The difficulty in attaining a fully saturated condition in the ECAP processing is a direct consequence of the much lower strains imposed on the billet during the processing operation.

5. Summary and conclusions

1. HPT and ECAP are both excellent methods for producing significant grain refinement in bulk oxygen-free Cu. Measurements show the average grain size decreases both with increasing HPT turns and with increasing ECAP passes. However, the average grain size is smaller at ~510 nm in HPT after 10 turns compared with ~2.9 μm in ECAP after 8 passes.

2. Reasonable homogeneity is achieved in both HPT and ECAP at sufficiently high strains. Thus, processing oxygen-free Cu by HPT for 10 turns produces a well-defined saturation hardness of Hv ≈ 130 whereas processing this material by ECAP through 8 passes produces a hardness of Hv ≈ 115 which is close to, but probably does not fully correspond to, the saturation condition. The ease of attaining a saturation hardness in HPT is associated with the much higher strain imposed in the HPT processing.

3. The variations in microhardness values across HPT discs in the initial stages of deformation are related to the predicted variation in the equivalent predicted strain but the

microhardness becomes generally homogeneous over the whole surfaces of the HPT discs at high strains. In processing by ECAP the local variations in the microhardness values are relatively minor and randomly distributed over cross-sectional surfaces cut perpendicular to the pressing direction.

4. The samples processed by HPT and ECAP give similar plots when the hardness data are plotted against the estimated values of the equivalent strain.

Acknowledgments

This work was supported by the European Research Council under ERC Grant Agreement No. 267464-SPDMETALS and by the College of Technological Studies under the Public Authority for Applied Education and Training in Kuwait.

References

[1] R.Z. Valiev, R.K. Islamgaliev and T.G. Langdon // *Prog. Mater. Sci.* **45** (2000) 103.

[2] R.Z. Valiev, Y. Estrin, Z. Horita, T.G. Langdon, M.J. Zehetbauer and Y.T. Zhu // *JOM* **58**(4) (2006) 33.

[3] Y. Estrin and A. Vinogradov // *Acta Mater.* **61** (2013) 782.

[4] R.Z. Valiev, Y. Estrin, Z. Horita, T.G. Langdon, M.J. Zehetbauer and Y.T. Zhu // *JOM* **68** (2016) 1216.

[5] E.O. Hall // *Proc. Phys. Soc. B* **64** (1951) 747.

[6] N.J. Petch // *J. Iron Steel Inst.* **174** (1953) 25.

[7] T.G. Langdon // *Acta Mater.* **61** (2013) 7035.

[8] R.Z. Valiev and T.G. Langdon // *Prog. Mater. Sci.* **51** (2006) 881.

[9] A.P. Zhilyaev and T.G. Langdon // *Prog. Mater. Sci.* **53** (2008) 893.

[10] A.P. Zhilyaev, B.K. Kim, G.V. Nurislamova, M.D. Baró, J.A. Szpunar and T.G. Langdon // *Scripta Mater.* **46** (2002) 575.

[11] A.P. Zhilyaev, G.V. Nurislamova, B.K. Kim, M.D. Baró, J.A. Szpunar and T.G. Langdon // *Acta Mater.* **51** (2003) 753.

[12] J. Wongsa-Ngam, M. Kawasaki and T.G. Langdon // *J. Mater. Sci.* **48** (2013) 4653.

[13] C. Xu, M. Furukawa, Z. Horita and T.G. Langdon // *Mater. Sci. Eng. A* **398** (2005) 66.

[14] M. Prell, C. Xu and T.G. Langdon // *Mater. Sci. Eng. A* **480** (2008) 449.

[15] C. Xu, Z. Horita and T.G. Langdon // *Acta Mater.* **55** (2007) 203.

[16] C. Xu, Z. Horita and T.G. Langdon // *Acta Mater.***56** (2008) 5168.

[17] R.B. Figueiredo, M.T.P. Aguilar, P.R. Cetlin and T.G. Langdon // *Metall. Mater. Trans. A* **42A** (2011) 3013.

[18] M. Kawasaki, R.B. Figueiredo and T.G. Langdon // *Acta Mater.* **59** (2011) 308.

[19] C. Xu, Z. Horita and T.G. Langdon // *Mater. Trans.* **51** (2010) 2.

[20] Y. Estrin, A. Molotnikov, C.H.J. Davies and R. Lapovok // *J. Mech. Phys. Solids* **56** (2008) 1186.

[21] M. Kawasaki // *J. Mater. Sci.* **49** (2014) 18.

[22] K.J. Al-Fadalah, S.N. Alhajeri, A.I. Almazrouee and T.G. Langdon // *J. Mater. Sci.* **48** (2014) 4563.

[23] A.I. Almazrouee, K.J. Al-Fadalah, S.N. Alhajeri and T.G. Langdon // *Mater. Sci. Eng. A* **641** (2015) 21.

[24] Y. Huang, S. Sabbaghianrad, A.I. Almazrouee, K.J. Al-Faddah, S.N. Alhajeri and T.G. Langdon // *Mater. Sci. Eng. A* **656** (2016) 55.

[25] Y. Iwahashi, J. Wang, Z. Horita, M. Nemoto and T.G. Langdon // *Scripta Mater.* **35** (1996) 143.

[26] M. Furukawa, Y. Iwahashi, Z. Horita, M. Nemoto and T.G. Langdon // *Mater. Sci. Eng. A* **257** (1998) 328.

[27] R.B. Figueiredo, P.R. Cetlin and T.G. Langdon // *Mater. Sci. Eng. A* **528** (2011) 8198.

[28] R.B. Figueiredo, P.H.R. Pereira, M.T. Aguilar, P.R. Cetlin and T.G. Langdon // *Acta Mater.* **60** (2012) 3190.

[29] R.Z. Valiev, Y.V. Ivanisenko, E.F. Rauch and B. Baudelet // *Acta Mater.* **44** (1996) 4705.

[30] F. Wetscher, A. Vorhauer, R. Stock and R. Pippan // *Mater. Sci. Eng. A* **387**-389 (2004) 809.

[31] F. Wetscher, R. Pippan, S. Sturm, F. Kauffmann, C. Scheu and G. Dehm // *Metall. Mater. Trans. A* **37A** (2006) 1963.

[32] Z. Horita and T.G. Langdon // *Mater. Sci. Eng. A* **410-411** (2005) 422.

[33] J. Wongsa-Ngam, M. Kawasaki, Y. Zhao and T.G. Langdon // *Mater. Sci. Eng. A* **528** (2011) 7715.

[34] Z. Horita, T. Fujinami, M. Nemoto and T.G. Langdon // *Metall. Mater. Trans. A* **31A** (2000) 691.

[35] C. Xu and T.G. Langdon // *J. Mater. Sci.* **42** (2007) 1542.

[36] S.N. Alhajeri, N. Gao and T.G. Langdon // *Mater. Sci. Eng. A* **528** (2011) 3833.

[37] J. Wongsa-Ngam, M. Kawasaki and T.G. Langdon // *Mater. Sci. Eng. A* **556** (2012) 526.

[38] C. Xu, Z. Száraz, Z. Trojanová, P. Lukáč and T.G. Langdon // *Mater. Sci. Eng. A* **497** (2008) 206.

[39] C. Xu, M. Furukawa, Z. Horita and T.G. Langdon // *Acta Mater.* **53** (2005) 749.

[40] A. Vorhauer and R. Pippan // *Scripta Mater.* **51** (2004) 921.

[41] S. Sabbaghianrad and T.G. Langdon // *Mater. Sci. Eng. A* **596** (2014) 52.

[42] S. Sabbaghianrad and T.G. Langdon // *J. Mater. Sci.* **50** (2015) 4357.

Figure captions

Fig. 1 Average microhardness values and average grain size for samples processed by (a) HPT and (b) ECAP.

Fig. 2 Colour-coded contour maps of the hardness measurements recorded over the surfaces of oxygen-free copper discs processed by HPT for (a) 1/4, (b) 1, (c) 5 and (d) 10 turns.

Fig. 3 Colour-coded contour maps of the hardness measurements recorded over the cross-sectional surfaces of oxygen-free copper billets processed by ECAP for (a) 1, (b) 2, (c) 4 and (d) 8 passes.

Fig. 4 Measured microhardness values plotted against equivalent strain for samples processed by (a) HPT and (b) ECAP.

a)

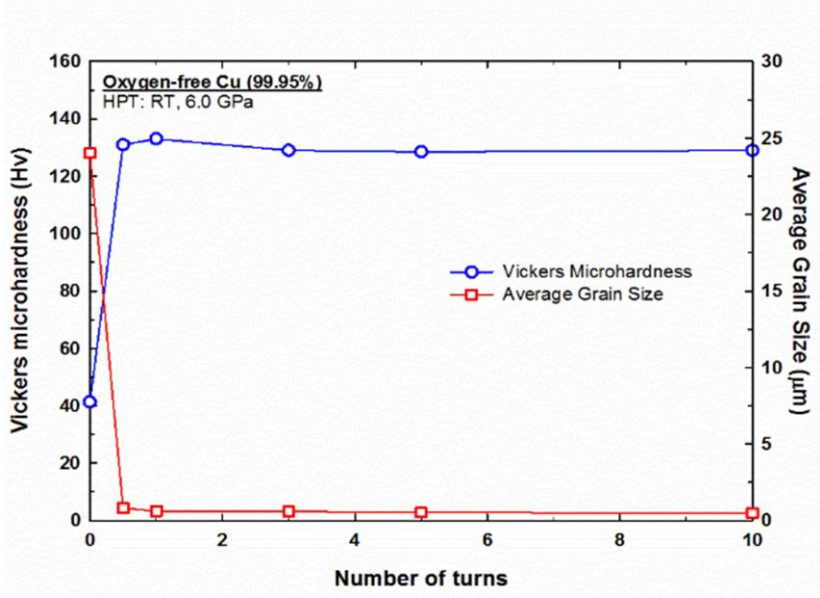

b)

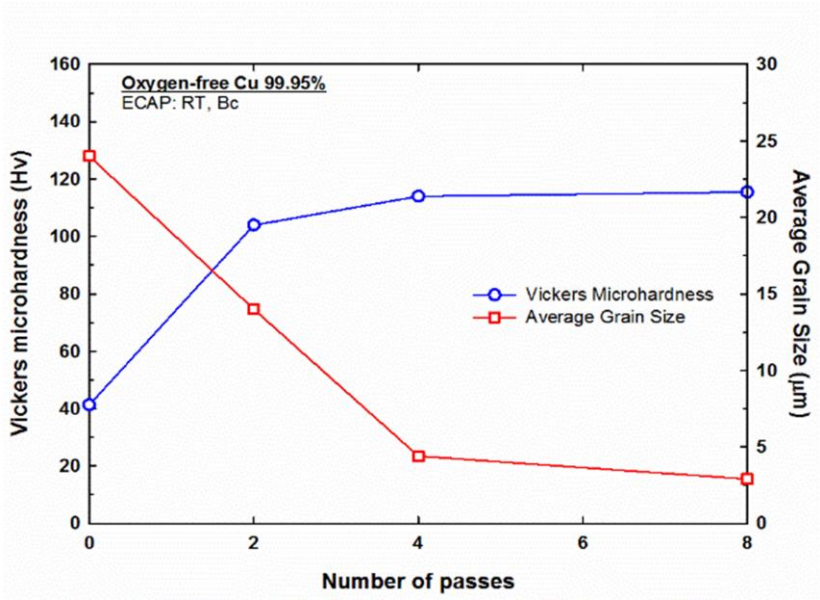

Fig. 1 Average microhardness and average grain size for samples processed by a) HPT and b) ECAP.

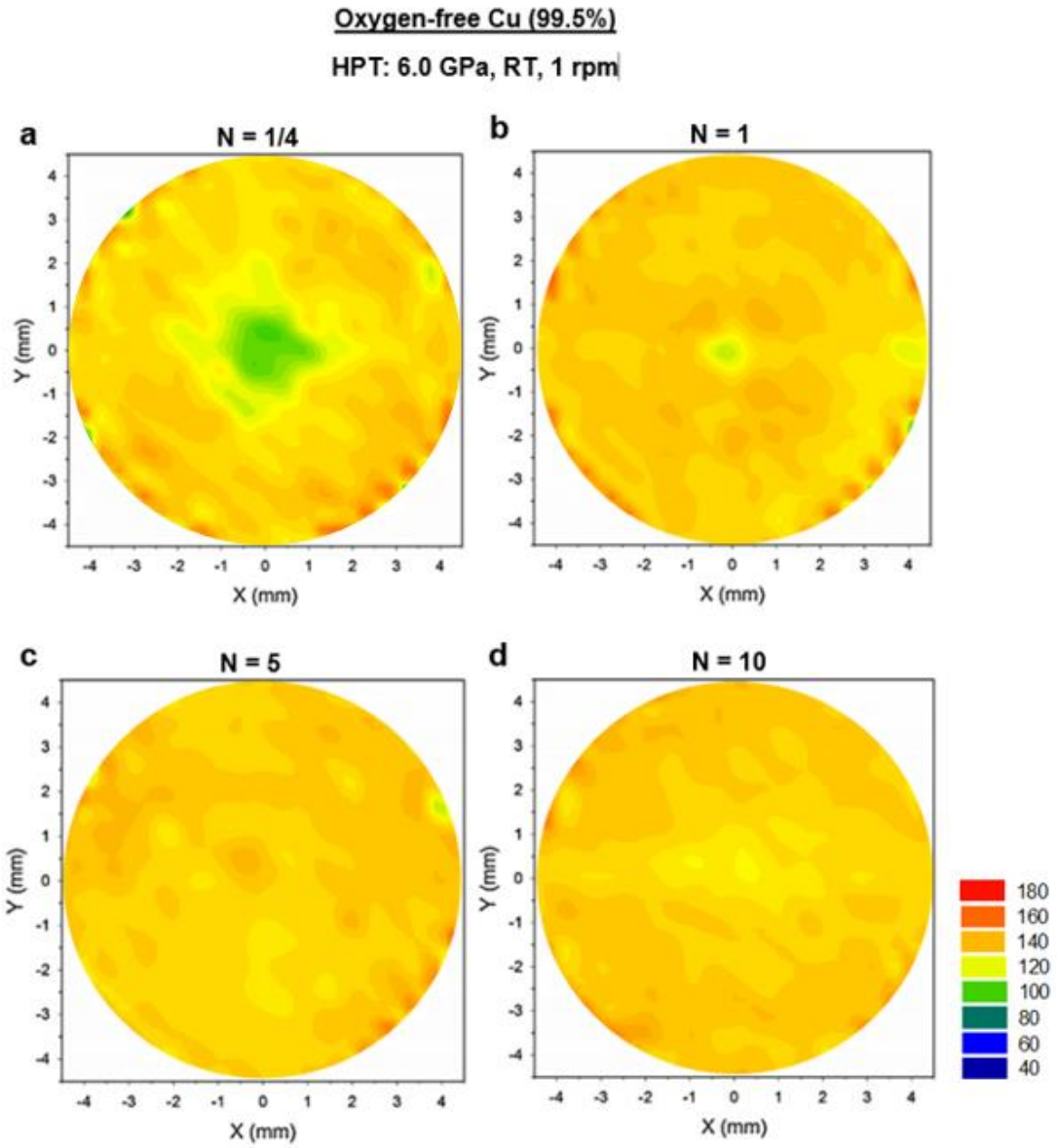

Fig. 2 Colour-coded contour maps of the hardness measurements recorded over the surfaces of oxygen-free copper discs processed by HPT for: (a) N = 1/4 ; (b) N = 1; (c) N = 5; and (d) N = 10.

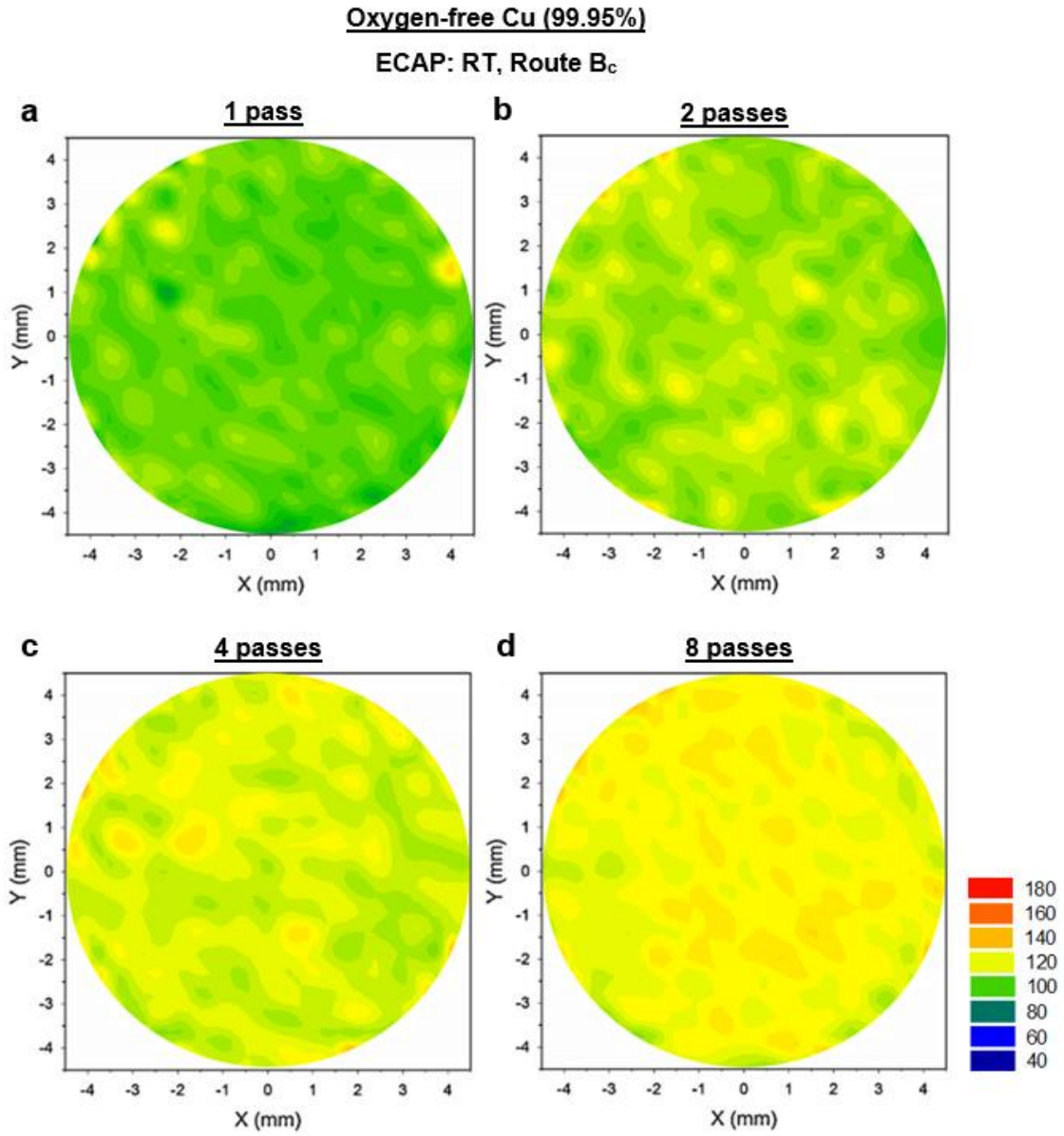

Fig. 3 Colour-coded maps showing the distribution of microhardness over the cross-sectional planes of oxygen-free copper discs processed by ECAP for (a) 1; (b) 2; (c) 4; and (d) 8 passes.

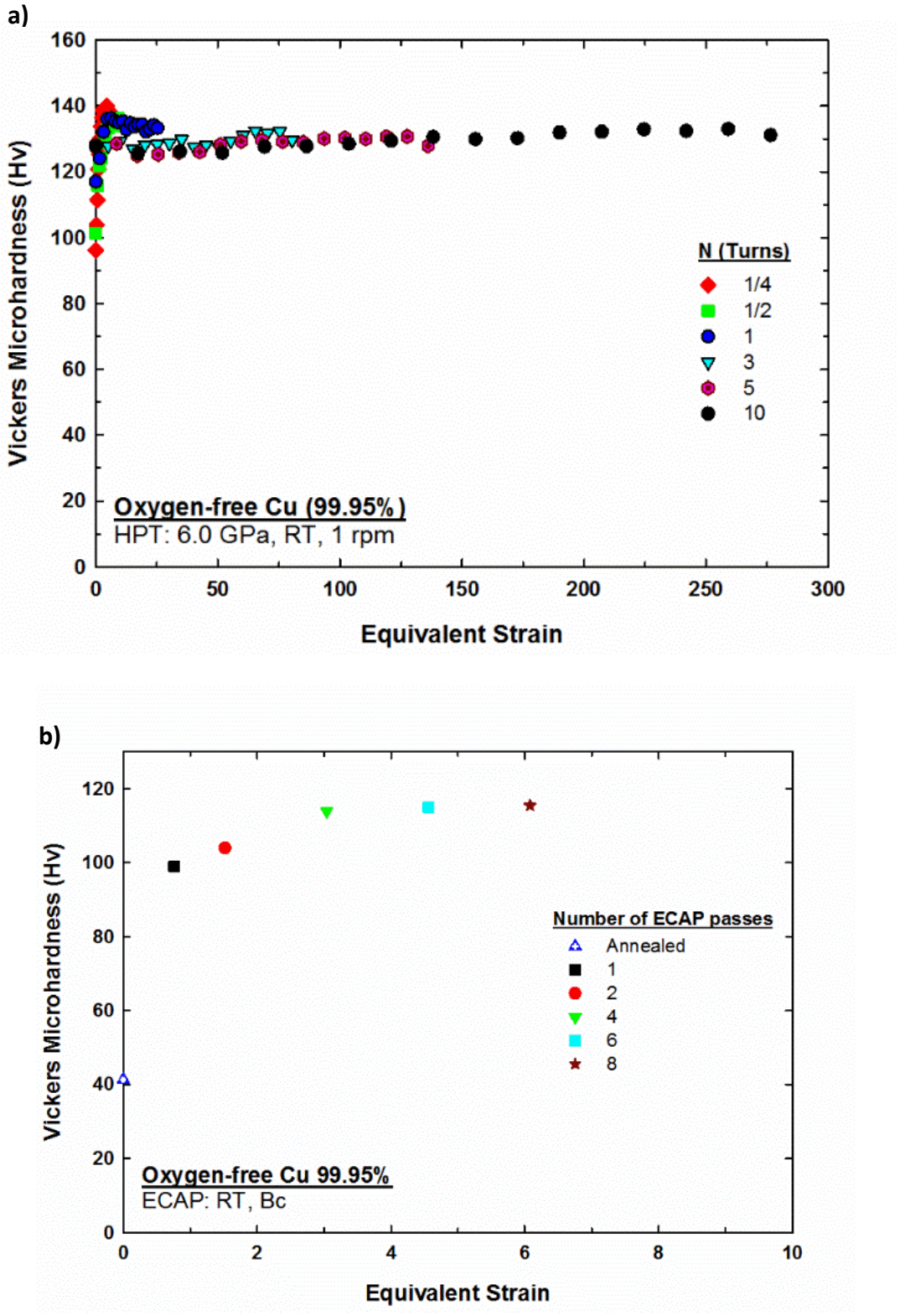

Fig. 4 Measured microhardness values plotted against equivalent strain for samples processed by a) HPT and b) ECAP.